University of Delaware
Newark, De 19716-3820
Ph: 302/831-6200
Fax: 302/831-6226
www.udel.edu/iec

INSTITUTE OF ENERGY CONVERSION

UNITED STATES DEPARTMENT OF ENERGY
UNIVERSITY CENTER OF EXCELLENCE
FOR PHOTOVOLTAIC RESEARCH AND EDUCATION

February 1, 2007

Bolko von Roedern
National Renewable Energy Laboratory
1617 Cole Boulevard
Golden, CO 80401

Re: NREL Subcontract #ADJ-1-30630-12
D.5.11

Dear Bolko,

This report covers research conducted at the Institute of Energy Conversion (IEC) for the period of December 16, 2006 to January 15, 2007, under the subject subcontract. The report highlights progress and results obtained under Task 3 (Si-based Solar Cells) and Task 4 (Process Diagnostics).

Task 3: Silicon based Solar Cells

Rear junction Solar Cells

Rear junction, all rear contact solar cells have several advantages over the more common front junction solar cell with contacts on either side. The advantages range from performance (no shading loss and avoiding the trade-off between series resistance and reflectance), manufacturability (for example, ease of series connection for module and allowing for higher packing factor) and aesthetic (a more uniform appearance PV module which is desirable for architectural applications).

THE UNIVERSITY OF DELAWARE IS AN EQUAL OPPORTUNITY UNIVERSIT

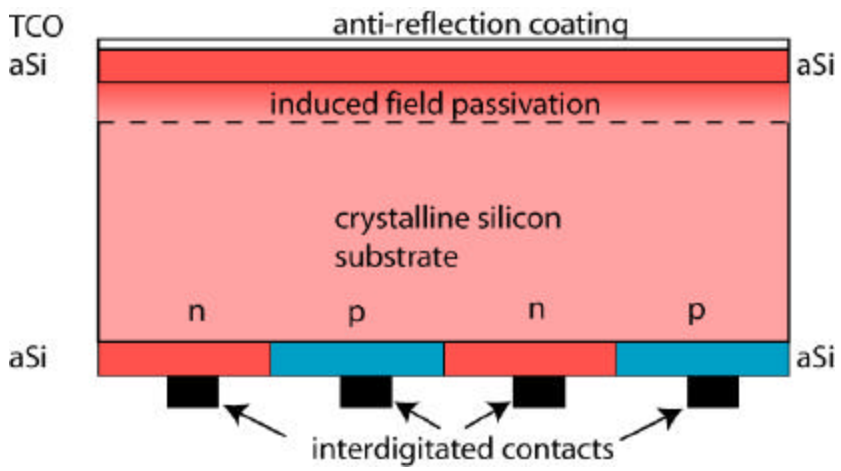

Figure 1: A rear junction design takes full advantage of the flexibility provided by deposited layers

While the advantages of rear junctions are well known, their implementation is hindered by several design constraints, which can be circumvented by amorphous silicon on crystalline silicon heterojunctions. Figure 1 shows a device with p and n a-Si contacts and emitters on the rear of a Si wafer. The front surface has a passivation layer and AR coating. There are at least three advantages of such a design. First, since rear junction cells require diffusion lengths greater than twice the device thickness, thin wafers are attractive. Using low temperature a-Si depositions rather than diffusions prevents bending of such wafers. Second, rear junction designs require low front surface recombination velocities which is provided by deposited passivation layers. Finally, the central challenge in rear junction solar cells, patterning the rear, is easier in silicon heterojunctions since it is much easier to mask and etch depositions than diffusions and further isolation between p/n a-Si layers is not always necessary. In addition, rear junction devices eliminate the front transparent-conductive-oxide (TCO) along with its absorption losses. This is particularly attractive since the recent rise in the cost of indium (a component in ITO) is a problem with current heterojunction technology.

The two-dimensional modeling program DESSIS has been used to design the optimum device for the rear contact structure. The calculations show that efficiencies of 22 % are possible using commercial Czokralski silicon substrates and levels of passivation already demonstrated at IEC.

Present Device Fabrication

Photolithography is the most flexible approach to implement proof-of-concept rear junction cells. It allows a relatively straightforward method to explore process variations while maintaining control over the process sequence. The goal of using the photolithographic approaches is to demonstrate the feasibility of rear junction solar cells and to develop an understanding of the dominant physical processes. The basic feasibility

of the approach has been demonstrated by initial results shown in Figure 2. These results indicate the potential of the basic device concept being investigated at IEC. Increased V_{OC} can be expected with optimization of the passivation (there was no intrinsic a-Si layer between the silicon and a-Si doped layer) and increased J_{SC} with a more transparent front passivation layer and AR coating.

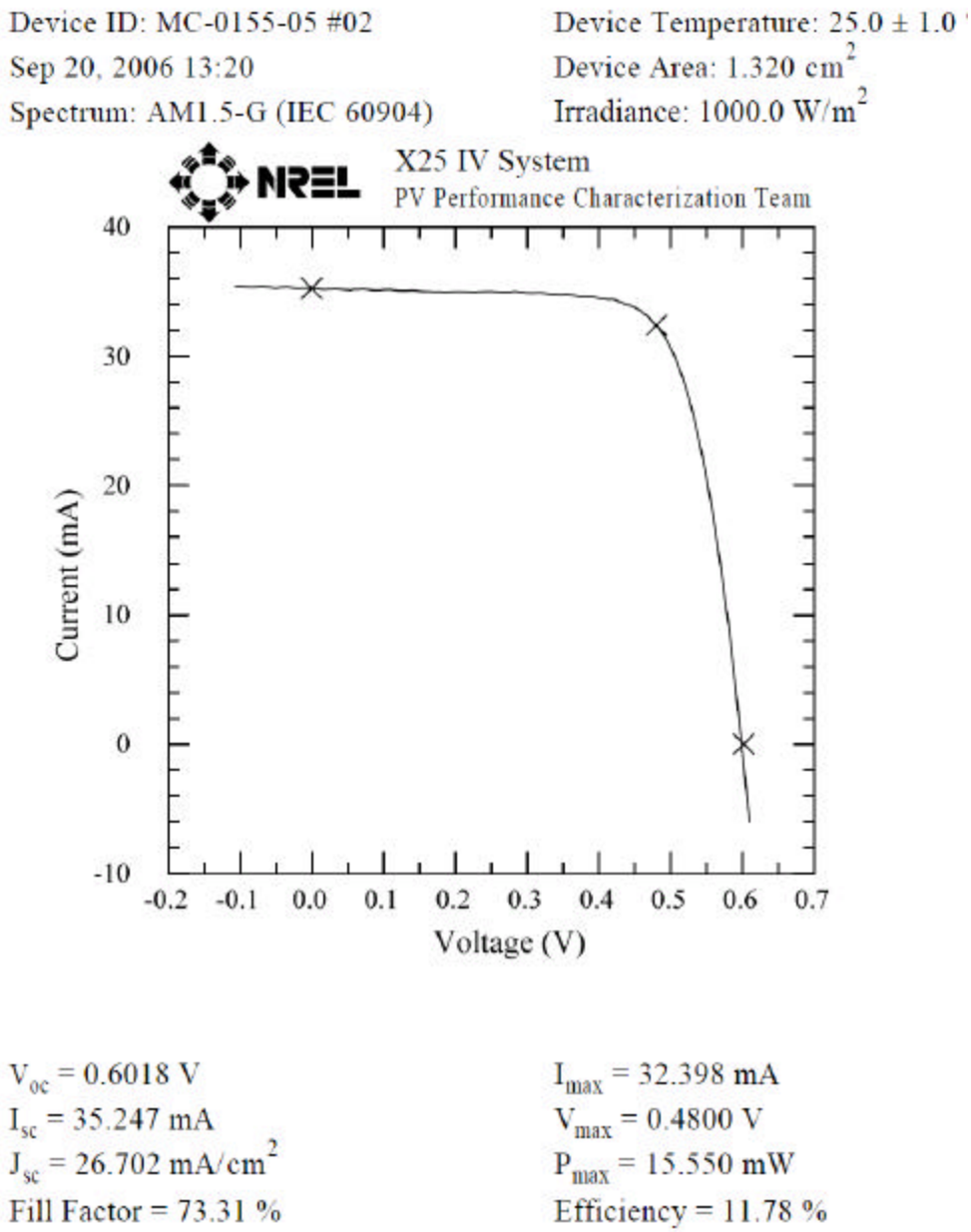

Figure 2: NREL confirmed efficiency of a rear junction cell.

High Open Circuit Voltage (V_{OC}) Cell

The device reported in the previous section was fabricated without the use of an intrinsic amorphous silicon buffer layer. The absence of the buffer layer makes it easier to fabricate the device and ensures a high fill factor but results in high recombination at the amorphous silicon/crystalline silicon interface. We have shown that much higher V_{OC}'s are attainable if an intrinsic buffer layer is inserted between the doped a-Si and the c-Si substrate. For example, on standard front junction devices at IEC we have obtained 703 mV with an intrinsic buffer layer but only 622 mV without the buffer layer. However, a disadvantage of inserting the intrinsic buffer layer is that it can reduce conduction of carriers and lead to low fill factors.

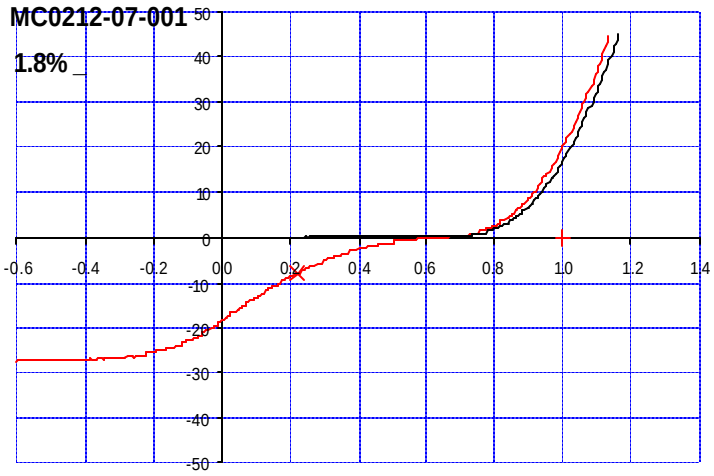

Figure 3: JV Curve of a rear junction cell with the addition of an intrinsic buffer layer. The cell has a high V_{OC} of 678 mV but the unoptimised i-layer gives a low fill factor.

The JV curve shown in Figure 3 is typical of a cell with an unoptimized i-layer between the doped layers and Si wafer. Poor conduction across the layer is reducing the fill factor and hence the efficiency. The measured V_{OC} of 678 mV shows the potential of the structure and compares favorably with the 681 mV obtained by Sunpower on their record rear junction device.

There is a high likelihood of improving the factor on this class of devices. Front junction cells fabricated at IEC initially had the same problem of very low fill factors. However, optimization of the i-layers enabled the fill factors on the front junction devices to exceed 70 %.

TASK 4: Process Diagnostics

Effusion Rate and Flux Distribution Estimation using Direct Simulation Monte Carlo Technique

Transitional flow conditions are usually encountered in the pilot-scale as well as commercial scale sources employed for CIGS film deposition. Direct Simulation Monte Carlo (DSMC) is a computational Monte Carlo algorithm for the stochastic simulation of rarefied gas flows, which is applicable for molecular regime flow to continuous flow. It is particularly suited for transitional flow regime, where both wall collisions and intermolecular collisions play an important role in determining flow characteristics. The primary assumptions for DSMC method are listed below:

- Particle motion and inter-particle collisions are decoupled over small time intervals.
- Particle motions are modeled deterministically.
- Collisions are treated statistically.
- Each simulated particle represents a large number of actual particles.
- Physical space is divided into "cells" of fixed volume; particles located within a given cell are allowed to interact.
- Average within a cell provides macroscopic flow properties at the center of the cell.

The effusion rate as well as vapor flux distribution depends to a great extent on the nozzle geometry. The transition flow equations which are typically used to describe the effusive flow characteristics, therefore, have to be experimentally fitted to the measured data. Specifically, the entrance loss factor parameter has to be experimentally determined for a given source and nozzle design, which can be prohibitive when different nozzle geometries and source dimensions have to be explored. To this extent, the DSMC technique is used to describe the effusive flow characteristics so as to remove the need for experiments. The simulation results are presented below.

The DSMC simulations considered here are three-dimensional in nature, where the one quarter of the source around the nozzle acts as the simulation physical space. The simulation parameters and the relevant assumptions are the following:

Simulation parameters:

- Number of simulated particles ~ 1000.
- Actual atoms per simulated particle: F ~ 1011.
- Initially all the particles are on the melt surface.

- Cubic cell with dimension: ?/3, *?: mean free path.*
- Time interval, ? t = t/10, *t: mean collision time.*
- Particles per cell = 30.

Assumptions:

- Uniform temperature throughout the physical space.
- The vapor effusion properties depend on the melt temperature directly below the nozzle.

The two critical effusive flow properties which we wish to estimate are:

1. *Vapor flow rate*, which is given by the number of particles exiting the nozzle per unit time

$$f = 4\frac{N_{out}FM}{N_A t}$$

where, N_{out} is the total number of particles that have exited the nozzle, N_A is the Avogadro number, t is the elapsed time, and M is the molecular weight of the species considered (copper).

2. *Angular flux distribution*, which is obtained from frequency distribution of the angles at which the particles exit the nozzle.

The simulation results for effusion rate and flux distribution are compared with the experimental data in Figures 4 and 5 respectively. DSMC simulation vapor flow rate prediction matches very well with the experimental data. Thus, DSMC simulation instead of real experiments can be used to determine vapor flow rates. This will greatly reduce the cost and development time for the process scale-up. DSMC angular distribution result also matches with experimental data really well. Furthermore, it can be seen that the $\cos^{n1}(\theta)+\cos^{n2}(\theta)$ relationship better describes the flux distribution better than the typically used $\cos^{n}(\theta)$.

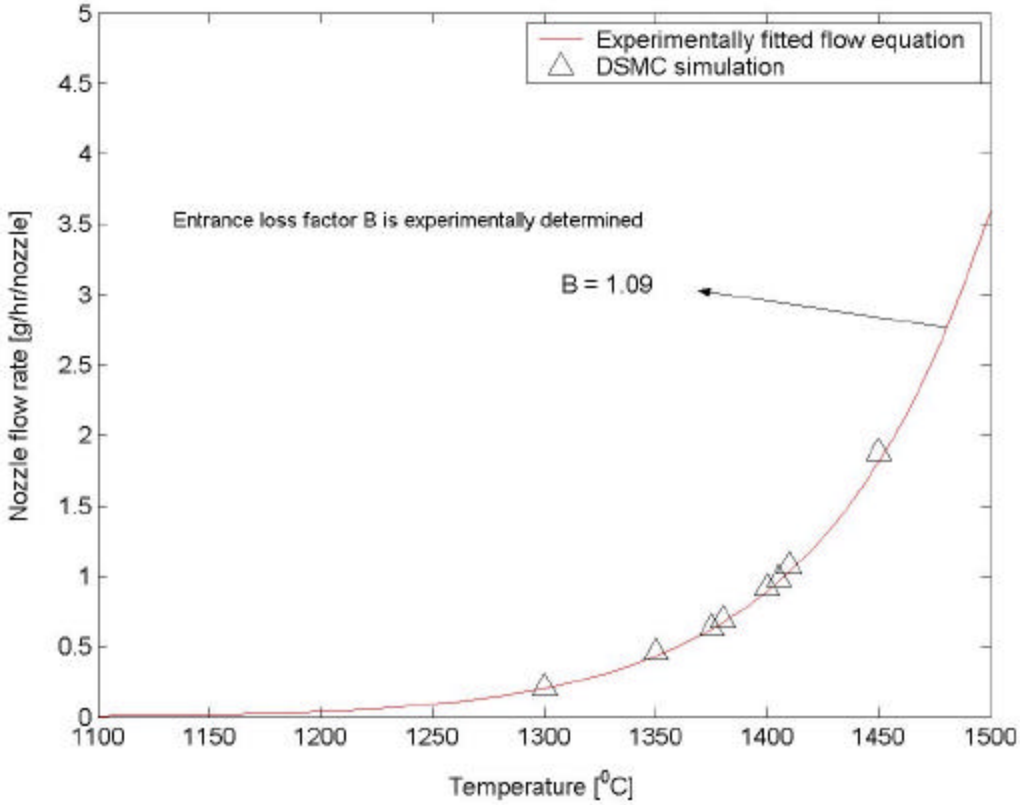

Figure 4: Effusion rate versus temperature plot: Experimentally fitted transitional flow equations are compared with the DSMC simulation results.

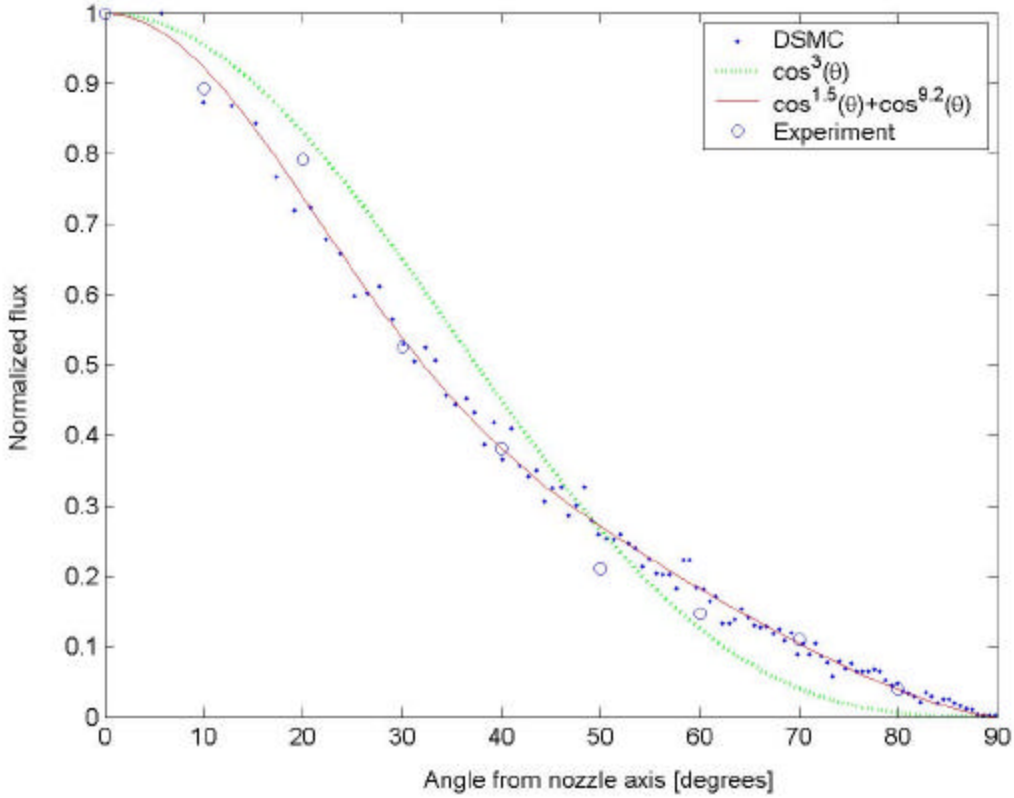

Figure 5: Vapor flux distribution plot: DSMC result is compared to experimental data and cosine power law.

Best regards,

Robert W. Birkmire
Director

CC: Paula Newton, IEC
Susan Tompkins, OVPR, UD
Carolyn Lopez, NREL